

# From the warm magnetized atomic medium to molecular clouds

Hennebelle P.<sup>1</sup>, Banerjee R.<sup>2</sup>, Vázquez-Semadeni E.<sup>3</sup>, Klessen R.<sup>2</sup>, Audit E.<sup>4</sup>

<sup>1</sup> Laboratoire de radioastronomie, UMR 8112 du CNRS,

École normale supérieure et Observatoire de Paris, 24 rue Lhomond, 75231 Paris cedex 05, France

<sup>2</sup> Zentrum fuer Astronomie der Universitat Heidelberg, Institut fuer Theoretische Astrophysik, 69120 Heidelberg, Germany

<sup>3</sup> Centro de Radioastronomía y Astrofísica, Universidad Autónoma de México, Apdo Postal 3-72 Morelia, 58089, México

<sup>4</sup> Service d'Astrophysique, CEA/DSM/DAPNIA/SAP, Centre d'Études de Saclay, l'Orme les Merisiers, 91191 Gif-sur Yvette Cedex, France

Preprint online version: October 31, 2021

## ABSTRACT

**Context.** It has recently been proposed that giant molecular complexes form at the sites where streams of diffuse warm atomic gas collide at transonic velocities.

**Aims.** We study the global statistics of molecular clouds formed by large scale colliding flows of warm neutral atomic interstellar gas under ideal MHD conditions. The flows deliver material as well as kinetic energy and trigger thermal instability leading eventually to gravitational collapse.

**Methods.** We perform adaptive mesh refinement MHD simulations which, for the first time in this context, treat self-consistently cooling and self-gravity.

**Results.** The clouds formed in the simulations develop a highly inhomogeneous density and temperature structure, with cold dense filaments and clumps condensing from converging flows of warm atomic gas. In the clouds, the column density probability density distribution (PDF) peaks at  $\sim 2 \times 10^{21} \text{ cm}^{-2}$  and decays rapidly at higher values; the magnetic intensity correlates weakly with density from  $n \sim 0.1$  to  $10^4 \text{ cm}^{-3}$ , and then varies roughly as  $n^{1/2}$  for higher densities.

**Conclusions.** The global statistical properties of such molecular clouds are reasonably consistent with observational determinations. Our numerical simulations suggest that molecular clouds formed by the moderately supersonic collision of warm atomic gas streams.

**Key words.** Magnetohydrodynamics (MHD) – Instabilities – Interstellar medium: kinematics and dynamics – structure – clouds

## 1. Introduction

The formation of molecular clouds is one of the key steps for the star formation process. A large number of studies investigate the internal dynamics of molecular clouds (e.g. see the review by MacLow & Klessen 2004), but only a few investigations address the problem of their formation itself (e.g. see the review by Hennebelle, Mac Low & Vázquez-Semadeni 2008). This is partly due to the difficulty in treating the large range of spatial scales relevant in this problem and partly due to uncertainties on the mechanisms at the origin of their formation. During the last decade, the idea has emerged that the molecular clouds may be formed at the onset of a large scale converging flow of atomic gas (e.g. Ballesteros-Paredes et al. 1999) with the active role of thermal instability (Hennebelle & Pérault 1999, Koyama & Inutsuka 2000, 2002, Audit & Hennebelle 2005, Heitsch et al. 2005, Vázquez-Semadeni

et al. 2006). Indeed, since the density of molecular clouds is much larger than the mean ISM density, large scale flows are a viable explanation to excite density enhancements. The origin of these flows is however unclear and may be not unique. Most likely they arise from turbulent fluctuations or gravitational instability occurring at large scales.

Recently large multi-dimensional non-magnetic numerical simulations have been performed (Hennebelle & Audit 2007, Vázquez-Semadeni et al. 2007, Heitsch et al. 2008, the last two including self-gravity) with the aim of studying in detail the formation of dense gas from a large flow of warm neutral medium, resolving down to the star forming scales.

In this letter, we present the first results of large adaptive mesh refinement (AMR), MHD simulations performed with the codes RAMSES (Teyssier 2002, Fromang et al. 2006) and FLASH (Fryxell et al. 2000). These are the first simulations which, starting from the WNM, include magnetic field, cooling, self-gravity, and thanks to the AMR scheme, have sufficient spatial resolution to resolve indi-

vidual, high density, clouds. The molecular clouds we observe in these simulations are self-consistently generated by thermal instabilities, turbulence and gravitational contraction. We stress that the internal structure and the turbulent properties of these molecular clouds are not the result of an ad hoc assumption on the external turbulent driving. By performing these numerical simulations, we expect to tackle unsolved and outstanding questions such as what drives turbulence in molecular clouds; what is the gas density and temperature distribution, and what is the structure of the magnetic field in these objects? In this letter we report on the most important global properties of the clouds. In subsequent articles (Banerjee et al. 2008), we will give a more detailed analysis of the cloud formation, structure and evolution, and on the efficiency of star formation in the simulations.

In section 2, we describe the numerical set up and the initial conditions whereas in section 3 we present our results and preliminary comparisons with observations. Section 4 concludes this paper.

## 2. Numerical setup and initial conditions

The numerical simulation presented in this letter has been performed with the AMR code RAMSES using the HLL solver. Ramses is a second order Godunov scheme and uses the constraint transport method to ensure  $\text{div}B = 0$  (see Fromang et al. 2006). Starting with an initial resolution of  $256^3$  cells, 2 levels of refinement are allowed during the calculation leading to an effective  $1024^3$  numerical simulation. The criterion used to refine the grid is a simple density threshold of  $50 \text{ cm}^{-3}$  for the first level and  $200 \text{ cm}^{-3}$  for the second one. This ensures that the dense gas is uniformly resolved. With the box size being about 50 pc, this leads to a spatial resolution of about 0.05 pc. The total number of cells in the simulation is about  $\simeq 4 \times 10^7$ . About 25,000 timesteps have been performed for a total of 30,000 cpu hours.

To mimic a large scale converging flow (e.g. Audit & Hennebelle 2005), a converging velocity field is imposed at the left and right faces of the simulation box, on top of which velocity modulations have been superimposed. The velocity of each incoming flow is twice the sound speed of the WNM, leading to a total velocity difference of about  $40 \text{ km s}^{-1}$  within the box. The amplitude of the modulation is about a factor of two, and it is periodic with a spatial frequency of 10 pc. The boundary conditions are periodic for the 4 remaining faces. Initially, the density and temperature are respectively  $1 \text{ cm}^{-3}$  and about 8000 K, which are also the values imposed at the left and right faces. The velocity is initially equal to zero through the box. The magnetic field is uniform initially and parallel to the x-axis, therefore aligned with the incoming velocity field and has an intensity of about  $5 \mu\text{G}$ , corresponding to equipartition between magnetic and thermal pressure initially. The cooling is due to atomic species as described in Audit & Hennebelle (2005). Molecular cooling and  $\text{H}_2$  formation are not treated at this stage. As we will see, this

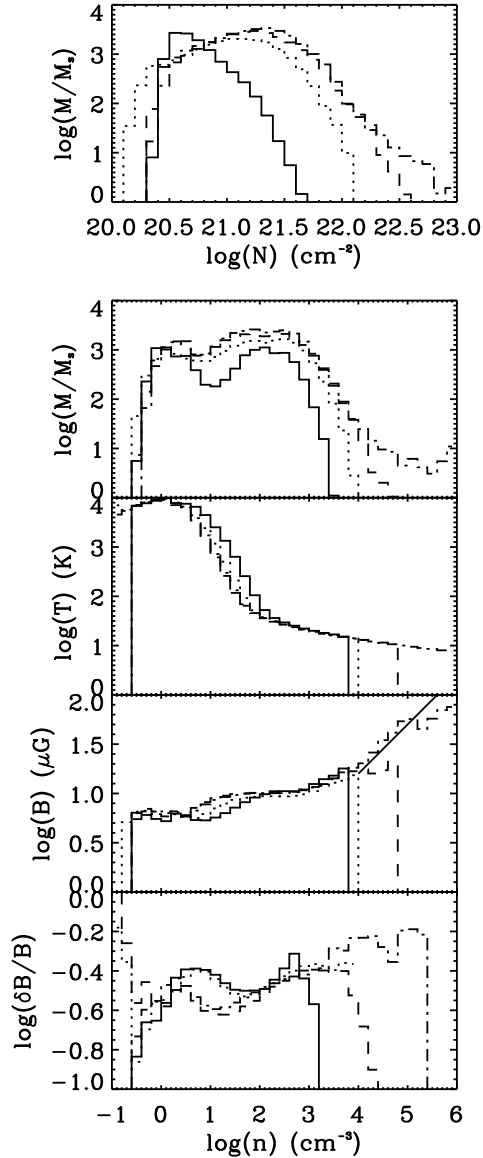


**Fig. 1.** Top and second panels: Column density and density PDF in the simulation. Third, fourth and fifth panels: Temperature, magnetic intensity and magnetic intensity variance as a function of gas density. The *solid*, *dotted*, *dashed*, and *dash-dotted* lines show the distributions at times  $t = 3.7, 7.7, 12.0$  and  $13.8$  Myr, respectively. The straight line in the fourth panel shows a distribution proportional to  $n^{1/2}$ .

nevertheless leads to reasonable temperature and density distributions.

## 3. Results

Figure 1 shows the column density and density pdf as well as temperature, magnetic intensity and its variance as a function of density at time 3.71, 7.7, 12 and 13.79 Myr. Because of the mass injection, the total mass increases

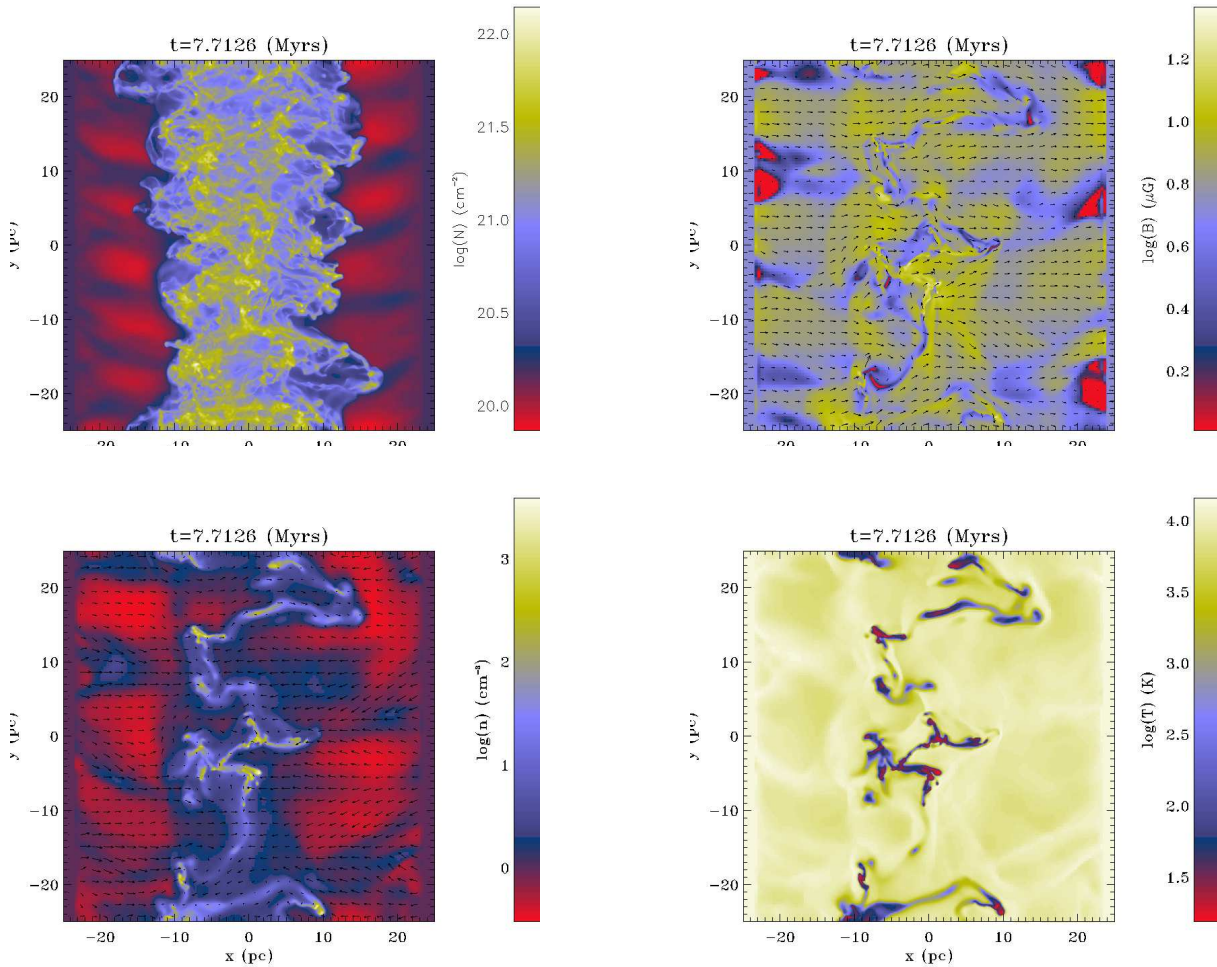


**Fig. 2.** Top left panel: column density. Top right panel: Magnetic intensity and its xy-components (indicated as arrows) in the  $z = 0$  plane. Bottom left panel: density and velocity fields in the  $z = 0$  plane. Bottom right panel: temperature in the  $z = 0$  plane.

continuously within the simulation box from about  $3000 M_s$  initially to roughly 10 times this value at time 13.79 Myr. At time 3.71 and 7.7 Myr, the largest density reached in the simulation is between a few times  $10^3 \text{ cm}^{-3}$  and  $10^4 \text{ cm}^{-3}$ , whereas at time 13.79 Myr gravity has taken over and triggers gravitational collapse producing much higher densities. This indicates that the cloud should start forming stars roughly 12 Myr after the collision of the converging flow has occurred ( $t \simeq 1$  Myr in the simulation). At later times, the cloud keeps forming stars while the total mass continues to increase. This is qualitatively in good agreement with the observations reported by Blitz et al. (2007) for the LMC, that the masses of GMCs with little star formation activity are smaller than those of GMCs with strong activity. We note that the duration of 7 Myr, they infer for the first massive starless phase, is similar to the timescale of our simulation roughly estimated between time 7.7 Myr and 13.79 Myr. We stress, however, that precisely defining the “birth” time of the molecular cloud in our simulation is an elusive task since the mass

is an increasing function of time. In future papers we will address this point from an observational perspective.

The mass weighted PDF of the column density distribution peaks at about  $2 \times 10^{21} \text{ cm}^{-2}$  and drops rapidly for higher values. It is interesting to note that this is similar to what has recently been inferred by Goldsmith et al. (2008) for the Taurus molecular cloud (see their figure 8).

The temperature drops rapidly for densities between 3 and  $30 \text{ cm}^{-3}$  where it reaches a value of about 50 K. It then slowly decreases down to about 10 K for densities higher than  $10^4 \text{ cm}^{-3}$ . Note that since UV shielding and molecular cooling are not considered here, the temperature in the dense gas is probably overestimated. This would imply that the average density of the cold clumps should probably be a little higher. Explicitly treating  $\text{H}_2$  formation would have the same effect (Glover & MacLew 2007).

For densities smaller than  $\simeq 1000 \text{ cm}^{-3}$ , the magnetic intensity increases very smoothly with density whereas for density larger than  $\simeq 1000 \text{ cm}^{-3}$ , it is roughly propor-

tional to  $\sqrt{\rho}$ . Indeed, the lower density gas is magnetically sub-critical and mainly flows along the magnetic field lines without compressing magnetic flux. On the other hand, the high density gas is supercritical and the magnetic flux is compressed along with the dense gas under the influence of the gravitational force. Future studies will have to investigate whether ambipolar diffusion modifies this behaviour significantly. The variance of the magnetic intensity increases smoothly with density and ranges from about one third to half the mean magnetic intensity. We note that this magnetic intensity distribution appears to be very similar to what has been inferred from observations (Troland & Heiles 1986, Crutcher 1999)

Figure 2 shows the column density along the  $z$ -axis, the density and velocity field at  $z = 0$ , and the temperature field in the same plane at time  $t = 7.7$  Myr after the beginning of the simulation. The column density reveals that the cloud has a complex internal structure made of filaments and dense clumps of density between  $100$ - $1000$   $\text{cm}^{-3}$ , embedded in a more diffuse phase. This is even more clearly apparent in the density and temperature cuts which show that the clumps are relatively isolated and embedded into the warm diffuse phase. This suggests that the molecular clouds are not homogeneous isothermal media, but rather, consist of a complex array of filaments and clumps, with denser gas being colder, and therefore with little or no excess of thermal pressure over the surrounding gas.

Interestingly, the density of the warm gas embedded in the molecular cloud is higher than in the outer medium ( $n \simeq 1$   $\text{cm}^{-3}$ ) and can be as large as  $3$ - $4$   $\text{cm}^{-3}$ . Indeed, this gas has been previously shocked and it is in the process of cooling as it moves towards the dense cold regions (Vázquez-Semadeni et al. 2006; Hennebelle & Audit 2007). From a comparison between the column density and temperature distribution in the  $z = 0$  plane, we note that the warm gas is deeply embedded in the molecular cloud. Note that in this work, the UV field is assumed to be constant. Although this is obviously not a good assumption for the dense gas, we see that since the filling factor of the cloud appears to be small, this is certainly a fair assumption for the WNM even when it is deeply embedded inside the cloud. Moreover, the higher temperatures are sometimes found at the edge of the clumps at the onset of the accretion shocks which occurs when the WNM flow encounters a dense clump. This clearly indicates that the dissipation of mechanical energy plays an active role in the heating of the warm phase. Altogether, this is in good agreement with the picture proposed by Hennebelle & Inutsuka (2006) except that the mechanical energy which heats the warm phase is the kinetic energy of the shocks rather than the energy of the MHD waves (possibly underestimated in this work since the ion-neutral drift is not treated). Note that the finding of interclump medium being low density atomic hydrogen ( $n < 4 - 10$   $\text{cm}^{-3}$ ) is consistent with the estimate of Williams et al. (1995) for the Rosette molecular cloud.

Figure 2 also shows the magnetic intensity in the  $z = 0$  plane as well as its  $xy$ -components. In the external medium the magnetic field remains much more uniform than in the dense regions, where its direction fluctuates significantly. Since the field was initially uniform, this implies that the turbulent motions are able to significantly distort the field.

## 4. Conclusion

We have presented the results of AMR MHD simulations aiming to describe self-consistently the formation of a molecular cloud from a converging flow of warm diffuse atomic hydrogen. Our simulations suggest a complex multi-phase structure of the molecular clouds which consists of cold and dense clumps embedded into a warm atomic phase. The simulations reproduce reasonably well the observed variations of magnetic intensity with density and column density distribution. Finally, we suggest that star formation may start in the cloud while it is still accreting material. This would imply that the mass of GMCs vary with time, in good agreement with recent observations (Blitz et al. 2007), and with the results of previous non-magnetic simulations of the phenomenon.

## References

- Audit, E., & Hennebelle, P. 2005, *A&A* 433, 1  
 Ballesteros-Paredes, J., Vázquez-Semadeni, E., & Scalo, J. 1999a, *ApJ*, 515, 286  
 Banerjee, R., Vázquez-Semadeni, E., Hennebelle, P., Klessen, R., 2008, *A&A*, in preparation  
 Blitz, L., Fukui, Y., Kawamura, A., Leroy, A., Mizuno, N., & Rosolowsky, E. 2007, in *Protostars and Planets V.*, eds. B. Reipurth, D. Jewitt, & K. Keil (Tucson: U. of Arizona Press) 81.  
 Crutcher, R., 1999, *ApJ*, 520, 706  
 Fromang, S., Hennebelle, P., Teyssier, R., 2006, *A&A*, 457, 371  
 Glover, S. C. O. G., & Mac Low, M.-M. 2007b, *ApJ*, 659, 1317  
 Goldsmith, P., Heyer, M., Narayanan, G., Snell, R., Li, D., Brunt, C., 2008, arXiv:0802.2206  
 Hennebelle, P., Mac Low, M.-M., & Vázquez-Semadeni 2007, in *Structure Formation in the Universe: Galaxies, Stars, Planets*, ed. G. Chabrier (Cambridge: Cambridge University Press), in press (arXiv:0711.2417)  
 Heitsch, F., Burkert, A., Hartmann, L., Slyz, A., & Devriendt, J. 2005, *ApJ* 633, 113  
 Heitsch, F., Hartmann, L., Slyz, A., Devriendt, J., & Burkert, A. 2008, *ApJ* 674, 316  
 Hennebelle, P., & Audit, E. 2007, *A&A*, 465, 431  
 Hennebelle, P., & Pérault, M. 1999, *A&A* 351, 309  
 Hennebelle, P., Inutsuka, S.-I. 2006, *ApJ*, 647, 404  
 Koyama, H., Inutsuka, S. 2000, *ApJ* 532, 980  
 Koyama, H., Inutsuka, S. 2002, *ApJ* 564, L97  
 Mac Low, M.-M., Klessen, R. S. 2004, *Rev. Mod. Phys.*, 76, 125  
 Fryxell, B., Olson, K., Ricker, P., et al. 2000, *ApJS*, 131, 273  
 Teyssier, R., 2002, *A&A*, 385, 337  
 Troland, T., & Heiles, C. 1986, *ApJ*, 301, 339

- Vázquez-Semadeni, E., Gómez, G. C., Jappsen, A. K.,  
Ballesteros-Paredes, J., González, R. F., & Klessen, R. S.  
2007, *ApJ*, 657, 870
- Vázquez-Semadeni, E., Ryu, D., Passot, T., González, R., &  
Gazol, A. 2006, *ApJ*, 643, 245
- Williams, J., Blitz, L., & Stark, A. 1995, *ApJ*, 451, 252